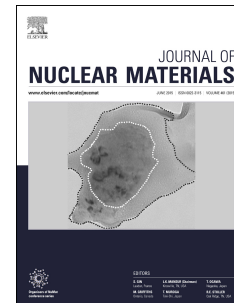


Accepted Manuscript

Effect of radial hydride fraction on fracture toughness of CWSR Zr-2.5%Nb pressure tube material between ambient and 300°C temperatures

Rishi K. Sharma, A.K. Bind, G. Avinash, R.N. Singh, Asim Tewari, B.P. Kashyap



PII: S0022-3115(18)30120-X

DOI: [10.1016/j.jnucmat.2018.06.003](https://doi.org/10.1016/j.jnucmat.2018.06.003)

Reference: NUMA 51016

To appear in: *Journal of Nuclear Materials*

Received Date: 26 January 2018

Revised Date: 20 May 2018

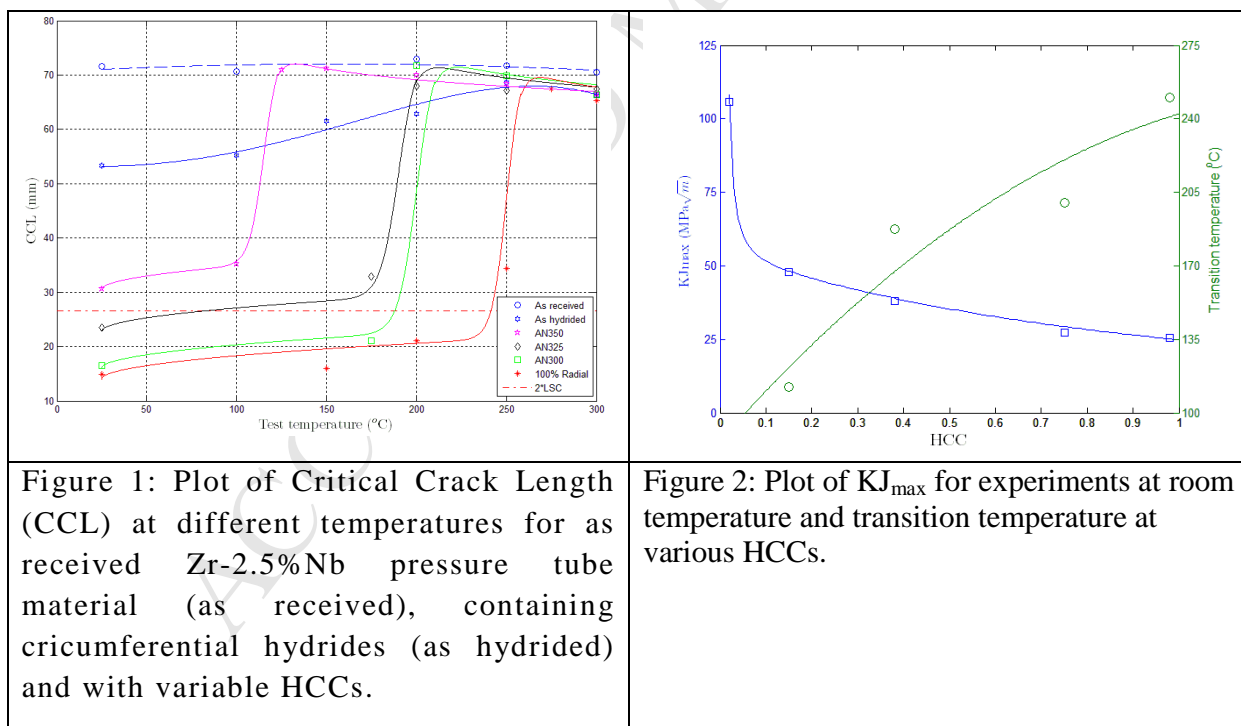
Accepted Date: 4 June 2018

Please cite this article as: R.K. Sharma, A.K. Bind, G. Avinash, R.N. Singh, A. Tewari, B.P. Kashyap, Effect of radial hydride fraction on fracture toughness of CWSR Zr-2.5%Nb pressure tube material between ambient and 300°C temperatures, *Journal of Nuclear Materials* (2018), doi: 10.1016/j.jnucmat.2018.06.003.

This is a PDF file of an unedited manuscript that has been accepted for publication. As a service to our customers we are providing this early version of the manuscript. The manuscript will undergo copyediting, typesetting, and review of the resulting proof before it is published in its final form. Please note that during the production process errors may be discovered which could affect the content, and all legal disclaimers that apply to the journal pertain.

Graphical abstract for the manuscript titled “**Influence of radial hydride fraction on fracture toughness of CWSR Zr-2.5%Nb pressure tube material between RT and 300 °C**” by Rishi K. Sharma, A. K. Bind, Avinash Gopalan, R. N. Singh, Asim Tewari and B. P. Kashyap has been prepared.

Fracture toughness of Zr-2.5%Nb alloy pressure tube material containing samples 100 wppm of hydrogen with variable radial hydride fraction was evaluated as per ASTM E1820-13 procedure between 25 and 300 °C. All the samples exhibited a sharp ductile brittle transition behavior and the transition temperature was observed to increase with increase in radial hydride fraction. The critical crack length (CCL) behavior with respect to the temperature for material containing hydrides of different HCC is presented in Fig.1. The CCL is calculated for 220 MWe pressure tube dimensions and maximum operating pressure. The CCL is calculated by iterative/recursion method with the formulation as described in CSA-N285.8-10. Fracture toughness properties were observed to improve after the annealing heat treatment due to the decrease in HCC as shown in Fig.2. The ambient temperature fracture toughness property was observed to be 105.7 MPa \sqrt{m} with 100 ppm circumferential hydrides and decreased rapidly to 49% with presence of 16.7% radial hydrides as presented in Fig.2. Further nearly linear reduction in the fracture toughness was observed with increase in radial hydride fraction. Ductile to brittle transition temperature in presence of radial hydrides was observed to increase with increase in HCC as shown in Fig.2.



ACCEPTED MANUSCRIPT

Effect of radial hydride fraction on fracture toughness of CWSR Zr-2.5%Nb pressure tube material between ambient and 300 °C temperatures

Rishi K. Sharma^{a,c}, A. K. Bind^b, Avinash G.^b R. N. Singh^{b*}, Asim Tewari^c, B. P. Kashyap^d

^aEngineering Directorate, Nuclear Power Corporation of India Limited, Mumbai-400094

^bMechanical Metallurgy Division, Bhabha Atomic Research Centre, Mumbai-400085

^cDepartment of Mechanical Engineering, Indian Institute of Technology Bombay, Mumbai-400076

^dDepartment of Materials Engineering, Indian Institute of Technology, Jodhpur, Karwad-342037

*Email: rnsingh@barc.gov.in, Tel. +91-22-25593817, FAX: +91-22-25505151

Abstract

Pressure tube spools fabricated from Zr-2.5%Nb alloy, were subjected to gaseous hydrogen charging and stress reorientation treatment to form radial hydrides in a specially designed fixture. Curved Compact Tension specimens of 17 mm width containing 100 wppm of hydrogen were made using electro discharge machining. Some of the samples were annealed at 300, 325 and 350 °C followed by furnace cooling. Metallographic examination of the samples revealed 100% radial hydride in the samples to which stress reorientation treatment was imparted. The radial hydride fraction decreased with increase in the temperature of annealing that followed stress reorientation. Fracture toughness of samples with variable radial hydride fraction was evaluated as per ASTM E1820-13 procedure between 25 and 300 °C. All the samples exhibited a sharp ductile to brittle transition behavior and the transition temperature was observed to increase with increase in the radial hydride fraction.

Keywords: Zr-2.5%Nb alloy, Pressure tube, Stress reorientation of hydrides, Radial hydrides, Hydride continuity coefficient (HCC), Fracture Toughness and Hydride Embrittlement.

1. Introduction

The Zr-2.5%Nb alloy Pressure Tubes (PTs) are employed in present Pressurized Heavy Water Reactors (PHWRs). The suitable texture and microstructure to the pressure tubes is imparted during its fabrication to minimize life limiting diametrical creep during reactor operation. The basal poles of the HCP α -Zr grains in the PTs are predominantly oriented along the circumferential (~54%), radial (~43%) and axial (~3%) directions [1]. The pressure tubes possess such a strong texture that either circumferential hydrides or radial hydride platelets can only be precipitated [2-4]. Preferentially circumferential hydrides are formed under unstressed condition owing to the microstructure of the cold worked & stress relieved (CWSR) Zr-2.5%Nb alloy PT material. Radial hydrides get precipitated if the PTs containing hydrogen are cooled from the solutionizing temperature in the presence of hoop tensile stress greater than a critical value required for reorientation of hydrides [3-5]. The degree of embrittlement of Zirconium alloy due to presence of the hydride precipitates is adversely affected by the hydride platelet's orientations [5-8].

Several studies have been performed for the Zr-2.5%Nb alloy having predominantly circumferential hydrides, to identify the effect of hydrogen or circumferential hydrides on the tensile, impact and fracture behaviour [9, 10]. Evaluation of fracture properties of Zircaloy-2 PT material with respect to hydride continuity coefficient (HCC) and at different temperatures have been reported [7]. These studies used flattened specimens of un-irradiated Zircaloy-2 PT material for CANDU reactor [7]. Fracture properties of Zr-2.5%Nb CANDU PT material has been evaluated for various hydride morphologies having HCC values up to 0.57 [6]. Based on the reported threshold stress to precipitate radial hydrides in un-irradiated Zr-2.5%Nb PT material [3, 4], design of an experimental setup to experimentally produce radial hydrides was proposed by

Sharma et al. [5]. Using this setup, 100% radial hydrides were produced in the PT spools and its influence on fracture toughness of the PT material used in Indian PHWRs have been evaluated at various temperatures and compared with the reported values [5]. However, fracture behaviour of Zr-2.5%Nb alloy PT material as a function of HCC and temperature have not been investigated systematically, although they are requisite for the safety assessment of the PTs approaching the end of life. Various degrees of radial hydrides in PTs can develop as a result of improper rolling, accidental cooling under high pressure, blister formation, oxide nodule formation, presence of cracks etc. Understanding of fracture behavior of the Zr-2.5%Nb PT material containing different radial hydride fraction or the hydride continuity coefficient (HCC) will be helpful in safety assessment.

In view of the above, there is a need for evolving a method to generate various degrees of radial hydrides. This was achieved by subjecting the PT spools containing 100% radial hydrides to different annealing heat treatments between 300 and 350°C to obtain hydrides with varying HCCs. The fracture toughness properties of Zr-2.5%Nb PT material containing various degrees of radial hydrides was evaluated between ambient and 300 °C as a function of HCCs.

2. Methodology

2.1 Formation of Circumferential Hydrides

Circumferential hydrides are formed if as received Zr-2.5%Nb alloy PT spool is charged with hydrogen without any external stress [5]. For gaseous hydrogen charging the polished PT spool was heated in presence of pure hydrogen gas up to 363 °C in a predesigned hydrogen charging system [5, 11]. Polishing was carried out to remove the oxide layer. High dynamic vacuum ($\sim 10^{-3}$ Pa) in the system was achieved using a vacuum pump to prevent reformation of the oxide layer as it is a physical barrier for the hydrogen diffusion into the spool material [5, 11]. The system was isolated and the isochoric condition was achieved. The amount of hydrogen picked up by the PT material can be estimated from the difference between initial and final hydrogen partial pressures. Using this method, 200 mm long PT spool was charged with 100 wppm of hydrogen. The presence of hydrogen and hydride distribution in the PT spool after hydrogen charging was verified using inert gas fusion (IGF) technique and metallography, respectively [5].

2.2 Metallographic Analysis

Metallography of the hydrided material was carried out. The metallography coupons were sliced along circumferential-radial plane of the PT spool using slow speed diamond cutter and enclosed in epoxy with the help of steel ring. The metallographic samples were ground successively using emery papers up to 800 grit [5, 11]. Etching of the metallography samples was prerequisite to observe hydrides under optical microscope. The hydrided Zr-2.5%Nb alloy metallographic samples were swab etched for ~30 seconds using cotton soaked in a solution containing hydrofluoric acid, nitric acid and water having relative composition as 0.1, 0.45 and 0.45, respectively [5, 11].

2.3 Stress Reorientation Treatment and Annealing

Sharma et. al. [5] designed, fabricated and successfully used an experimental setup to precipitate 100% radial hydrides in the PT Spool. In this experimental setup the assembly containing hydrogen charged PT spool was put into universal testing machine (UTM). The UTM was employed with an environmental chamber, such that the setup can be heated up to a predefined temperature and then cooled in a controlled manner. More details of the experimental setup, details of rig used and the methodology for stress reorientation treatment can be found in Ref.[5]. In order to dissolve all the hydride precipitates, the PT spool was heated to solutionizing temperature (i.e. 400 °C) and soaked for 30 min. The PT spool was permitted to cool at 1 °C/min from the solutionizing temperature to 350 °C and it was soaked for 30 minutes. The plunger was

pushed into the PT spool inducing the threshold tensile hoop stress to form radial hydride precipitates [5]. The design of the setup was such that the threshold hoop stress of 200 MPa was maintained throughout the process and it does not exceed the yield strength of the material at all temperatures during the process [4, 5]. The PT spool was allowed to cool under the hoop stress in the environmental chamber to 150 °C and the load was removed [5]. The setup was cooled to room temperature in air.

Three sets of PT spools were made, from the stock spools having 100% radial hydrides by providing annealing heat treatments at 300 °C (AN300), 325 °C (AN325) and 350 °C (AN350) temperatures. For the annealing heat treatments of the PT spools, it was heated to the selected temperatures, soaked for an hour for homogenization, and then finally furnace cooled at the rate of 1 °C/min.

2.4 Hydride Continuity Coefficient (HCC)

Hydride continuity coefficient (*HCC*) was used to characterize the hydride morphology, orientation and distribution [12]. The *HCC* was affected by both the degree of reorientation and the total hydrogen content in the material. The value of *HCC* varied from 0 to 1. Low value signifies that few hydrides are present and/or hydrides are predominantly oriented in the circumferential direction. Contrary to this, high value of *HCC* represents the predominantly radial hydrides and high hydrogen content. For *HCC* calculation a band of size 2.5 mm in radial direction and 0.11 mm in circumferential direction was chosen as schematically shown in Fig.1 [12]. Ratio of radially projected length of all the hydrides and total band length is known as *HCC* [12]. The *HCC* calculations have been carried out for three random bands in a micrograph and mean value of the three was evaluated as bought out in Eqs.1-2 below:

$$HCC_i = \frac{HC_1 + HC_2 + HC_3 \dots}{L} \quad \dots (1)$$

$$HCC = \sum_{i=1}^3 \frac{HCC_i}{3} \quad \dots (2)$$

The HCC was determined for Zr-2.5%Nb alloy PT spools containing 100% radial hydrides subjected to appropriate annealing heat treatments.

2.5 Evaluation of Fracture Toughness

The curved compact toughness (CCT) specimens having 17 mm width (W) were made using electro discharge machining (EDM) from the PT spools containing hydrides with variable HCCs for evaluation of fracture toughness as shown in Fig.2a&2b. Fracture toughness parameters for CCT and flat CT specimens are evaluated using equations for flat CT specimen and compared for Zircaloy-2 and Zr-2.5%Nb PT material [13]. It has been reported that fracture toughness results from CCT and flat CT specimens are almost identical for the entire range of fracture toughness assessed [13]. The machining of the CCT specimens was carried out such that crack plane was set along the axial–radial plane and direction of crack propagation was kept along the axial direction of the PT spool as shown in Fig.2a. The testing and evaluation of fracture parameters from the CCT specimens was carried out as per the recommendations of the ASTM standard E-1820-13 [14]. In order to get sharp crack tip as a prerequisite for the fracture testing, fatigue pre-cracking the specimens was accomplished with the help of Rumul make resonance pre-cracker. The fatigue pre-cracking load was reduced in four equal steps from 500 N to 350 N, the ratio of maximum and minimum load was maintained as 10. The curvature of the CCT specimens can lead to non-uniform crack front along the specimen thickness and it can significantly affect the fracture parameters [14]. Predesigned tapered pins were used during the fatigue pre-cracking to

get the uniform crack extension across specimen thickness. The final crack size for the CCT specimen achieved post fatigue pre-cracking was designated as ‘ a ’, such that the ratio of crack size (a) and Width (W) ‘ a/W ’ was maintained around 0.5.

Fracture testing of the fatigue pre-cracked specimens was carried out using Zwick Roell made electro-mechanical universal testing machine (UTM). The test temperature was achieved by heating the specimens in air to desired elevated temperature using a three-zone furnace fitted on the UTM. The sample temperature was achieved within ± 1 °C during the experiment, with the help of three K-type (Chromel/Alumel) thermocouples, with the help of programmed temperature controller. The thermocouples were mounted at top, middle and bottom of the specimen to achieve uniform temperature. The fracture test starts after one hour soaking of the specimen at the test temperature.

The mode-I tensile load on the specimen was applied at a cross-head speed of 0.2 mm/min. Single specimen fracture testing required online monitoring of the crack growth. Crack growth during the test was observed with the help of Direct Current Potential Drop (DCPD) technique using a constant direct current source of 6 Amperes [10]. Platinum wires of 0.2 mm was spot welded within 1 mm on both side of the notch and DCPD output was recorded online during the test. Crack length at corresponding data point was evaluated by linearly interpolating the DCPD signals between two known crack lengths (initial and final). After completion of the test, initial and final crack lengths were measured by heat tinting of the specimens at 300 °C for 10 mins and subsequently tearing it apart. Nine point average method described in ASTM standard E-1820-13 [14] was followed for initial and final crack length measurements. Crack initiation point on DCPD signal was marked based on the deviation of the DCPD signal [15].

The J-integral parameter is a measure of energy required for crack growth under monotonic loading conditions and it can be divided into elastic part (J_{el}) and plastic part (J_{pl}) (ASTM standard E-1820-13 [14]) components as presented in Eq.3. The elastic part of the J-integral (J_{el}) for the current crack length $a(i)$ and load $P(i)$ were calculated using expression of K_I as shown in Eqs.4-6 below:

$$J(i) = J_{el}(i) + J_{pl}(i) \quad \dots(3)$$

$$J_{el}(i) = \frac{K_I^2(i)(1-\nu^2)}{E} \quad \dots(4)$$

$$K_I(i) = \frac{P(i)}{BW^{0.5}} f\left(\frac{a(i)}{W}\right) \quad \dots(5)$$

$$f\left(\frac{a(i)}{W}\right) = \frac{\left[2+\frac{a(i)}{W}\right]\left[0.886+4.64\frac{a(i)}{W}-13.32\left(\frac{a(i)}{W}\right)^2+14.72\left(\frac{a(i)}{W}\right)^3-5.6\left(\frac{a(i)}{W}\right)^4\right]}{\left(1-\frac{a(i)}{W}\right)^{3/2}} \quad \dots(6)$$

These values were estimated at numerous points along the loading curve. The Young’s modulus (E) and Poisson’s ratio (ν) of the material at various test temperatures (T) were calculated using $E = 95.9 - 57.4(T - 273)$ and $\nu = 0.436 - 4.8 \times 10^{-4}(T - 273)$, respectively [15, 16]. The corrected load line displacement was obtained by correcting for variation in compliance because of loading train assembly in line with ASTM standard E-1820-13 [14]. The area under the load v/s corrected load line displacement curve (A_{pl}) for a certain crack length represent the energy consumed during the plastic deformation of the specimen and crack extension. The plastic part of the J-integral (J_{pl}) was calculated using expressions given by Eqs.7-9, for the concurrent unbroken ligament $b(i)$:

$$J_{pl}(i) = \left[J_{pl}(i-1) + \frac{\eta(i-1)}{b(i-1)} \frac{(A_{pl}(i) - A_{pl}(i-1))}{B} \right] \left[1 - \gamma(i-1) \frac{(a(i) - a(i-1))}{b(i-1)} \right] \quad \dots(7)$$

$$\eta(i-1) = 2 + \frac{0.522b(i-1)}{w} \quad \dots(8)$$

$$\gamma(i-1) = 1 + \frac{0.76b(i-1)}{w} \quad \dots(9)$$

The expression $A_{pl}(i) - A_{pl}(i-1)$ in Eq.7 is representing the increment in the area of load v/s plastic load line displacement and was calculated by Eq.10:

$$A_{pl}(i) - A_{pl}(i-1) = \frac{(P(i-1) + P(i))(\delta(i-1) - \delta(i))}{2} \quad \dots(10)$$

J-integral versus the crack extension plot was obtained. The blunting line calculated by expression $J_{blunt} = 2\sigma_f(\Delta a)$, where σ_f is flow stress (mean of yield strength and ultimate tensile strength of the material) was superimposed over J v/s Δa plot. Exclusion lines were drawn at 0.15 mm and 1.5 mm crack extension. The empirical data between the two exclusion lines were approximated using power law function ($J = C_1 \Delta a^{C_2}$) and straight line fit. In a valid J-test, the J-integral parameter at the maximum load during the test was considered as J_{max} [14]. Slope of the best fit line is known as dJ/da . For some low ductility specimens, valid J test could not be performed due to pop-in behavior, for these specimens J_{max} was represented by J_{Kmax} as determined from Eq.11:

$$J_{Kmax} = \frac{K_{max}^2(1-v^2)}{E} \quad \dots(11)$$

The critical crack length (CCL) represents the crack length above which catastrophic failure of the PT under operating conditions will occur. The critical crack length ($CCL = 2c$) was computed by iterative technique for mean radius of the PT (r_m), thickness (w) and operating pressure (p) using Eq.12 [16]:

$$c = \frac{K_{max}^2 \pi}{8\sigma_f^2 \ln \left[\sec \left(\frac{\pi M \sigma_h}{2\sigma_f} \right) \right]} \quad \dots(12)$$

where, $M = \left[1 + 1.255 \left(\frac{c^2}{r_m w} \right) - 0.0135 \left(\frac{c^2}{r_m w} \right)^2 \right]^{1/2}$ and applied hoop stress $\sigma_h = p \left(\frac{r_m - 0.5w}{w} + 1 \right)$. CCL values obtained from iterative method is more conservative as compared to the one calculated from the graphical method [15]. This is because the use of J_{max} in the iterative method effectively truncates the J-R curve at smaller crack extensions and result in a smaller CCL [15].

3. Results

3.1 Formation of Circumferential and Radial Hydrides

The PT spools made from quadruple melted ingots charged with 100 wppm of hydrogen, showed predominantly circumferential hydrides (dark horizontal lines) [5]. The formation of predominantly circumferential hydrides is attributed to the microstructure of the CWSR Zr-2.5%Nb alloy PT material [17]. Circumferential-radial plane of the PT spool subjected to reorientation treatment showed 100% radial hydrides [5].

It was observed that the radial hydrides again got oriented back partially to circumferential direction, when subjected to annealing treatment at temperature greater than 300 °C. Optical micrographs after the annealing treatments of stress reoriented samples are shown in Fig.3a, Fig.3b and Fig.3c. As is evident from Figs.3(a-c), part of radial hydrides, which dissolved at the reorientation temperature precipitated back as circumferential hydrides after the specified annealing heat treatment. The HCC of these samples are listed in Table-1.

3.2 Fracture Toughness Evaluation in presence of Hydrides with different HCCs

The fracture toughness of this material with different HCCs was determined using samples made from the hydrogen charged Zr-2.5%Nb PT spools subjected to stress reorientation treatment followed by appropriate annealing heat treatment. Fracture toughness parameters were evaluated as per the ASTM standard E-1820-13 [14] at different temperatures between ambient and 300 °C temperatures. The load v/s load line displacement (LLD) curves for this material having circumferential and radial hydrides have shown different behavior especially temperature below the transition [5]. The load v/s LLD curves of the material containing hydrides with different HCCs are shown in Figs.4a-4c. At higher temperatures, high value of LLD was observed indicating higher resistance to crack growth. Contrary to this, for the samples having hydrides with high HCCs, the pop-in behavior representing lower toughness was seen at temperature below the transition.

The variation in maximum load toughness (KJ_{max}) at various test temperature for Zr-2.5%Nb alloy PT material having hydrides of different HCCs is shown in Fig.5. In view of the pop-in behavior detected at temperature below the transition for the samples with high HCC, the valid 'J' test could not be performed and hence the KJ_{max} shown in Fig.5 corresponds to K_{max} . The PT material containing fraction of radial hydrides clearly exhibit ductile to brittle transition behavior by exhibiting a typical S-curve dependence of fracture toughness on temperature. The KJ_{max} was nearly constant up to a certain temperature, increased with an increase in the test temperature over the transition region and then finally reached the saturation level at an upper shelf temperature (Fig.5). The transition behavior of the fracture toughness with temperature is predominantly visible for specimens with high HCCs. Minor reduction of the fracture toughness in the upper shelf region can be attributed to lowering of strength of the material at the high temperatures [5].

The CCL values at different temperatures for material containing hydrides of different HCC is shown in Fig.6. The CCL was calculated with respect to dimensions of 220 MWe PT of Indian PHWRs and at maximum operating pressure. For the evaluation of CCL iterative method [10, 15] was used using the formulation mentioned in CSA-N285.8-10 [16]. CCL calculation using the iterative method is found to be lower than the graphical method as in iterative method the J-R curve is truncated at a smaller crack extension [15]. Hence, iterative method deliver conservative CCL values for the Leak Before Break (LBB) qualification of the PTs [18]. CCL was nearly constant up to a temperature, found to be increasing sharply with the test temperature over the transition region and reached saturation at an upper shelf temperature (Fig.6). Transition behavior of the CCL with temperature is predominantly visible for specimens with high HCCs.

Fracture toughness properties were observed to improve after the annealing heat treatment due to the decrease in HCC as shown in Fig.7. The ambient temperature fracture toughness property was observed to be 105.7 MPa \sqrt{m} with 100 ppm circumferential hydrides and decreased rapidly to 49% with presence of 16.7% radial hydrides as presented in Table-1 and Fig.7. Further nearly linear reduction in the fracture toughness was seen with increase in radial hydride fraction. The presence of radial hydrides or high HCC, was found to increase the ductile to brittle transition temperature as shown in Fig.7.

3.3 SEM Fractography ACCEPTED MANUSCRIPT

SEM fractographs of fractured surface of PT material having hydrides of different HCCs and tested at ambient temperature are shown in Figs.8&9. Annealing of the samples at 300 °C resulted in marginal reduction in sample thickness near the crack tip. However, annealing of the samples at 350 °C resulted in significant reduction in sample thickness on the fracture plane, indicating that crack growth is accompanied by significant plastic deformation. Ductile tearing zones having micro-cavities were seen on the fractographs, representing ductile fracture behaviour of the parent material. The ductile tearing zones were observed to be larger in size and more frequent in distribution for the specimen containing the hydrides with lower HCC or lower radial hydride fraction. Conversely, the ductile tearing zones were observed to be smaller in size and less frequent in distribution for the specimen containing the hydrides with higher HCC indicating predominantly brittle fracture.

4. Discussion

The habit plane for the δ -hydride precipitates is observed to be along the basal plane of the single crystal α -Zr [19-22]. In view of this, it is more probable to form radial hydrides in unstressed condition for the textured PT material. Though, microstructure of the pressure tube facilitates precipitation of circumferential hydrides in the unstressed condition of Zr-2.5Nb alloy PT material. However, it tends to form radial hydrides if hoop stress more than a threshold is maintained while cooling from solutionizing temperature [4, 5]. The fracture properties of the Zr-2.5%Nb alloy PT material is significantly affected by the morphology of the hydride precipitates [5]. In the present study, systematic evaluation of fracture toughness properties for Indian CWSR Zr-2.5%Nb alloy PT material, for different HCCs and temperatures, have been carried out. Specimens containing variable radial hydride fraction were generated by providing appropriate annealing heat treatment to Zr-2.5%Nb alloy PT spools containing 100% radial hydrides [5].

4.1 Change in HCC with Annealing Heat Treatment

Annealing heat treatment to the PT spools containing 100% radial hydrides resulted into change in the fraction of radial hydrides as represented in Table-1. Hydride dissolution at the annealing heat treatment temperature depends on the terminal solid solubility for hydride dissolution (TSSD). Mean TSSD values for the cold worked Zr-2.5%Nb alloy PT material is reported in the Canadian standards [16]. The difference of the total hydrogen content and the TSSD at the annealing temperature is expected to represent the radial hydride fraction. The fraction of dissolved radial hydrides at the annealing heat treatment temperature is likely to nucleate as circumferential hydrides or contribute to the growth of pre-existing radial hydrides. A comparison of the radial hydride fraction determined metallographically and the difference between the total hydrogen content and TSSD at the annealing temperature is shown in Fig.10. It is observed that the reported mean TSSD [16] showed an excellent fit with the radial hydride fraction. For the annealing temperature of 300 °C, the mean TSSD is ~58.7 ppm, whereas the radial hydride fraction determined metallographically is 74.8%. This suggests that significant amount of dissolved hydrogen has contributed to the growth of pre-existing radial hydrides. However, for the higher annealing temperature of 350 °C, mean TSSD is about 105 ppm and hence entire amount of hydrogen is expected to be in solid solution at the annealing temperature. The radial hydride fraction determined metallographically is 12.8% suggesting the dissolved hydrogen has predominantly precipitated as circumferential hydrides but part of the dissolved hydrogen has precipitated as radial hydride due to memory effect. The data in Fig.10 shows that at 300 °C both the phenomenon were equally probable whereas at 350 °C, entire amount of hydrogen is expected to be in solid solution and during cooling predominantly circumferential hydrides formed with small fraction of radial hydride re-precipitating at pre-existing locations due to memory effect.

Hence, change in HCC with annealing heat treatment can be attributed to competition between the nucleation of circumferential hydrides and growth of pre-existing radial hydrides or memory effect.

4.2 Effect of HCC on Fracture Toughness

Presence of 100% radial hydrides in CWSR Zr-2.5%Nb alloy PT material significantly influence the fracture toughness and material transition behaviour [5]. The fracture toughness exhibits a weak dependency on temperature for the as-received (without additional hydrogen charging) material Zr-2.5%Nb alloy PT maetrial. Ductile to brittle transition behavior with respect to temperature having wider transition regime is seen for the material having circumferential hydrides [5]. The transition regime have been observed to be narrow for PT specimens containing 100% radial hydrides [5]. Zirconium alloy cladding material having equiaxed microstructure, containing radial hydrides, have shown reduced fracture resistance properties and crack growth through the void nucleation, growth and coalescence process at the crack tip [8].

Compared to as received material, presence of circumferential hydrides was found to lower the fracture toughness properties for all test temperatures [5]. Presence of radial hydrides further lower the fracture toughness properties of Zr-2.5%Nb PT material at all temperature below the transition [5]. Axial splitting followed by localized deformation for the sample containing circumferentail hydrides was observed to be the micro-mechanism for the crack growth [5]. SEM fractography of the as received PT maetrial shows ductile fracture surface and predominantly ductile fibrous zones on the fractured surface of PT material having circumferential hydrides [5].

Variation in HCC in the PT material affect the fracture toughness considerably [5-7]. Presence of 100% radial hydrides was found to significantly embrittles the PT material at lower temperatures and it follows a typical ‘S’ curve behaviour with sharp transition regime [5]. For the specimens tested at temperature more than the transition, the PT material shows fracture toughness similar to samples having circumferential hydrides [5]. At room temperature fracture toughness reduced to one fifth in presence of 100% radial hydrides than with the circumferential hydrides [5]. However, a systematic study to understand the effect of different HCCs on the fracture toughness was found to be missing.

The decrease in HCC by the annealing heat treatment, resulted in decrease in hydride size in radial direction and increase of the ligament between two radial hydrides. The large size ligament improves toughness of the material. The fracture toughness showed a ductile brittle transition behavior and the transition temperature was found to decrease with reduction in the HCCs. The fracture toughness of the PT material with limited number of radial hydrides were observed to be better or equivalent to the samples containing circumferential hydrides in the upper shelf region. This can be attributed to combined effect of change in stress profile due to partially dissolving hydrides [23] and torturous path of crack propagation in presence of both radial & circumferential hydrides.

SEM fractographs of the specimens with $HCC = 0.75$ and $HCC = 0.15$ tested at ambient temperature are as shown in Fig.8 and Fig.9, respectively. The bigger size ductile tearing zones in the fractographs indicate the ductile fracture behavior and higher toughness. The fracture surface revealed that the ductile fracture resulted from the big size and elongated dimples in the crack growth direction. This, in turn, suggests that the fracture is accompanied by the material plasticity and hence providing greater resistance to the crack growth.

4.3 Critical Crack Length (CCL)

Zr-2.5%Nb alloy PT material having radial hydrides with high HCC showed significantly low CCL values at room temperature. The present results show that, the PTs in presence of radial

hydrides having HCC=0.98, 0.75 and 0.38, the required safety factor of 2 on CCL for LBB qualification is not available at lower temperature and operating pressure, if upper bound leakage size crack (LSC) of 4 times of the wall thickness is considered [18]. However, as the HCC decrease further, the CCL value improves at ambient temperature, which also reduces the transition temperature. The observed dependency on temperature of the CWSR Zr-2.5%Nb alloy PT material containing hydrides of different morphology may have an effect on the pressurization procedure practiced while reactor startup or shutting down.

5. Conclusions

The present study of fracture toughness evaluation of Zr-2.5Nb pressure tube material containing 100 wppm hydrogen / hydrides with different HCCs lead to following main conclusions:

- i. Part of the radial hydrides were found to precipitate back as circumferential hydrides, when cooled from solution annealing temperatures in the absence of external stress suggesting radial hydride formation under stress is reversible. Annealing the pressure tube spools with 100% radial hydrides successfully produced variable radial hydride fraction or HCC.
- ii. The fracture toughness tests, accomplished at different temperatures between 25 and 300 °C on samples with variable HCCs, revealed that the increase in HCC reduces the ambient temperature fracture toughness gradually.
- iii. The variation in fracture toughness showed a typical ‘S’ curve representing ductile to brittle transition behavior. The transition temperature was observed to be decreasing with reduction in the HCCs. In the upper shelf region, the fracture toughness was observed to be independent of HCCs.
- iv. Smaller size and distant zones of ductile fracture were seen on the fracture surface of the samples containing radial hydrides. The size and density of these zones was observed to increase with decrease in HCC.

Acknowledgements

Constant encouragement provided by Mr. S. M. Ingole, AD, NPCIL, Mr. A. K. Balasubramanian, ED, NPCIL and Mr. U. C. Muktibodh, Director(T), NPCIL is acknowledged. Authors are grateful to Dr. G. K. Dey, former Director, Materials Group and Dr. Madangopal K., AD, Materials Group for the invaluable support in extending the use of experimental facilities. Thanks to Dr. K. V. Mani Krishna of MMD for his help in SEM examination of fracture surface. The help extended by Mr. Sandeep A. Chandanshive of MMD, BARC in hydrogen charging and metallography is also acknowledged.

References

- [1] R.N. Singh, S. Mukherjee, R. Kishore, B.P. Kashyap, Flow behaviour of a modified Zr–2.5wt%Nb pressure tube alloy, *Journal of Nuclear Materials* 345(2-3) (2005) 146-161.
- [2] R.N. Singh, S. Roychowdhury, V.P. Sinha, T.K. Sinha, P.K. De, S. Banerjee, Delayed hydride cracking in Zr–2.5Nb pressure tube material: influence of fabrication routes, *Materials Science and Engineering: A* 374(1-2) (2004) 342-350.
- [3] R.N. Singh, R. Kishore, S.S. Singh, T.K. Sinha, B.P. Kashyap, Stress-reorientation of hydrides and hydride embrittlement of Zr–2.5 wt% Nb pressure tube alloy, *Journal of Nuclear Materials* 325(1) (2004) 26-33.
- [4] R.N. Singh, R. Lala Mikin, G.K. Dey, D.N. Sah, I.S. Batra, P. Ståhle, Influence of temperature on threshold stress for reorientation of hydrides and residual stress variation across thickness of Zr–2.5Nb alloy pressure tube, *Journal of Nuclear Materials* 359(3) (2006) 208-219.
- [5] R.K. Sharma, S. Sunil, B.K. Kumawat, R.N. Singh, A. Tewari, B.P. Kashyap, Influence of hydride orientation on fracture toughness of CWSR Zr-2.5%Nb pressure tube material between RT and 300 °C, *Journal of Nuclear Materials* 488 (2017) 231-244.
- [6] A.C. Wallace, G.K. Shek, O.E. Lepik, Effects of Hydride Morphology on Zr-2.5Nb Fracture Toughness, *Zirconium in the Nuclear Industry*, ASTM STP 1023, 1989, pp. 66-88.
- [7] P.H. Davies, C.P. Stearns, Fracture Toughness Testing of Zircaloy-2 Pressure Tube Material with Radial Hydrides using Direct Current Potential Drop, *Fracture Mechanics*, ASTM STP 905, 1986, pp. 379-400.
- [8] K.S. Chan, X. He, Y.M. Pan, Fracture resistance of a zirconium alloy with reoriented hydrides, *Metallurgical and Materials Transactions A* 46(1) (2015) 58-71.
- [9] R.N. Singh, U.K. Viswanathan, S. Kumar, P.M. Satheesh, S. Anantharaman, J.K. Chakravartty, P. Ståhle, Influence of hydrogen content on impact toughness of Zr–2.5Nb pressure tube alloy, *Nuclear Engineering and Design* 241(7) (2011) 2425-2436.
- [10] R.N. Singh, A.K. Bind, N.S. Srinivasan, P. Stahle, Influence of hydrogen content on fracture toughness of CWSR Zr–2.5Nb pressure tube alloy, *Journal of Nuclear Materials* 432 (2013) 87-93.
- [11] R.N. Singh, R. Kishore, S. Mukherjee, S. Roychowdhury, D. Srivastava, T.K. Sinha, P.K. De, R. Kameswaran, S.S. Sheelvantra, B. Gopalan, S. Banerjee, Hydrogen Charging, Hydrogen Content Analysis and Metallographic Examination of Hydride in Zirconium Alloys, BARC report E034, 2003.
- [12] L.G. Bell, R.G. Duncan, Hydride Orientation in Zr-2.5%Nb; How it is affected by Stress, Temperature and Heat Treatment, AECL-5110, 1975.
- [13] C.K. Chow, L.A. Simpson, Determination of the fracture toughness of irradiated reactor pressure tubes using curved compact specimens, *Fracture Mechanics: Eighteenth Symposium*, ASTM STP 945, Philadelphia, 1988, pp. 419-439.
- [14] ASTM-Standards, Standard Test Method for Measurement of Fracture Toughness, ASTM E-1820, 2013.
- [15] A.K. Bind, R.N. Singh, H.K. Khandelwal, S. sunil, J.K. Chakravartty, A. Ghosh, P. Dhandharia, D. Bachawat, S. Vijayakumar, Fracture toughness evaluation of Zr-2.5Nb pressure tubes manufactured employing double forging for PHWR700, *Material Performance and Characterization* 3(3) (2014) 322-341.
- [16] CSA-N285.8-10, Technical requirements for in-service evaluation of zirconium alloy pressure tubes in CANDU reactors, D.13.3, Canadian Standard Association, 2010.
- [17] D.O. Northwood, U. Kosasih, Hydrides and Delayed Hydrogen Cracking in Zirconium and its Alloys, *International Metals Reviews* 28(2) (1983) 92-121.
- [18] G.D. Moan, C.E. Coleman, E.G. Price, D.K. Rodgers, S. Sagat, Leak before break in the Pressure Tubes of CANDU Reactors, *International Journal of Pressure Vessel & Piping* 43 (1990) 1-21.

- [19] R.K. Sharma, A. Tewari, R.N. Singh, B.P. Kashyap, Optimum shape and orientation of δ -hydride precipitate in α -zirconium matrix for different temperatures, Journal of Alloys and Compounds 742 (2018) 804-813.
- [20] R.N. Singh, P. Stahle, L. Banks-Sills, M. Ristmanaa, S. Banerjee, δ -Hydride Habit Plane Determination in α -Zirconium at 298 K by Strain Energy Minimization Technique, Defect and Diffusion Forum 279 (2008) 105-110.
- [21] D.G. Westlake, The Habit Planes of Zirconium Hydride in Zirconium and Zircaloy, Journal of Nuclear Materials 26 (1968) 208-216.
- [22] K. Une, K. Nogita, S. Ishimoto, K. Ogata, Crystallography pf Zirconium Hydrides in Recrystallized Zircaloy-2 Fuel Cladding by Electron Backscatter Diffraction, Journal of Nuclear Science and Technology 41(7) (2004) 731-740.
- [23] R.N. Singh, H.K. Khandelwal, A.K. Bind, S. Sunil, P. Stähle, Influence of stress field of expanding and contracting plate shaped precipitate on hydride embrittlement of Zr-alloys, Materials Science and Engineering: A 579 (2013) 157-163.

Figure 1: Schematic of band on radial-circumferential plane and details of calculations for hydride continuity coefficient (HCC)

Figure 2: Schematic depicting (a) orientation of CCT specimens wire cut from Zr-2.5%Nb PT spool and (b) details of CCT specimens

Figure 3: Optical micrograph depicting hydride morphology along radial-circumferential plane of Zr-2.5%Nb alloy PT spool after charging 100 wppm of hydrogen, subjected to stress reorientation and annealing heat treatment for 1 hour at (a) 300 °C, (b) 325 °C and (c) 350 °C temperature.

Figure 4a: [AN300] Load vs. LLD curves of samples having partial radial hydride (stress reorientation treatment + annealing at 300 °C for 1 hour) and tested between 25 °C and 300 °C temperature. Pop-in was seen for the samples tested up to 175 °C.

Figure 4b: [AN325] Load vs. LLD curves of samples having partial radial hydride (stress reorientation treatment + annealing at 325 °C for 1 hour) and tested between 25 °C and 300 °C temperature. Pop-in was seen for the samples tested up to 175 °C.

Figure 4c: [AN350] Load vs. LLD curves of samples having partial radial hydride (stress reorientation treatment + annealing at 350 °C for 1 hour) and tested between 25 °C and 300 °C temperature. Pop-in was seen for the samples tested up to 100 °C.

Figure 5: Behavior of fracture toughness ($K_{J_{max}}$) with respect to temperature for as received Zr-2.5%Nb alloy PT material (as received), having circumferential hydrides (as hydrided) and having hydrides with variable HCCs (100% Radial, AN300, AN325 and AN350).

Figure 6: Critical Crack Length (CCL) behavior with respect to temperatures for as received Zr-2.5%Nb alloy PT material (as received), having circumferential hydrides (as hydrided) and having hydrides with variable HCCs (100% Radial, AN300, AN325 and AN350).

Figure 7: Plot of room temperature fracture toughness ($K_{J_{max}}$) and transition temperature with respect to different HCCs.

Figure 8: SEM fractographs of Zr-2.5%Nb alloy PT material having partial radial hydrides (AN300) for fracture testing at ambient temperature. Crack growth direction is from left to right. Small size and distant zones of ductile tearing were seen on the fracture surface (a) lower magnification and (b) higher magnification.

Figure 9: SEM fractographs of Zr-2.5%Nb alloy PT material having partial radial hydrides (AN350) for fracture testing at room temperature. Crack growth direction is from left to right. Big size and densely populated zones of ductile tearing features were seen on the fracture surface (a) lower magnification and (b) higher magnification.

Figure 10: Plot of fraction of radial hydride and (total hydrogen content – TSSD) for various annealing heat treatment temperatures

List of Tables:

Table 1: Hydride continuity coefficient (HCC) and fraction of radial hydride after stress reorientation treatment and annealing heat treatments of pressure tube spools having 100 wppm of hydrogen

Table 1: Hydride continuity coefficient (HCC) and fraction of radial hydride after stress reorientation treatment and annealing heat treatments of pressure tube spools having 100 wppm of hydrogen

Condition	HCC	Fraction of radial hydrides (%)
As hydrided	0.02	0
After stress reorientation treatment (100% Radial)	0.98	100
Stress reorientation + Heat treatment at 300 °C (AN300)	0.75	74.91
Stress reorientation + Heat treatment at 325 °C (AN325)	0.38	47.73
Stress reorientation + Heat treatment at 350 °C (AN350)	0.15	12.59

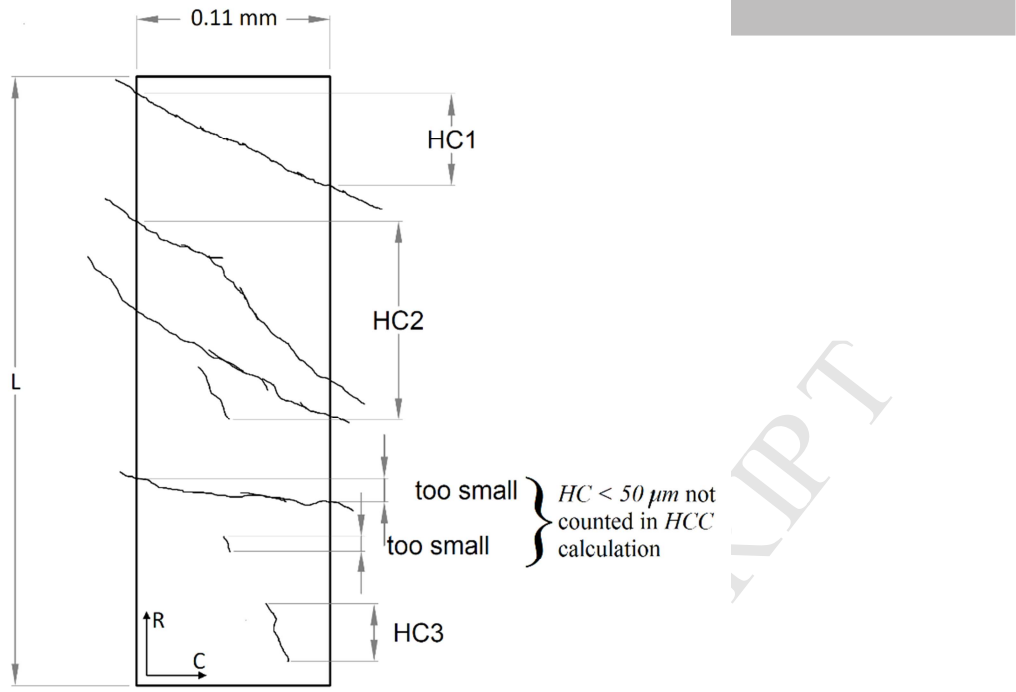


Figure 1: Schematic of band on radial-circumferential plane and details of calculations for hydride continuity coefficient (HCC)

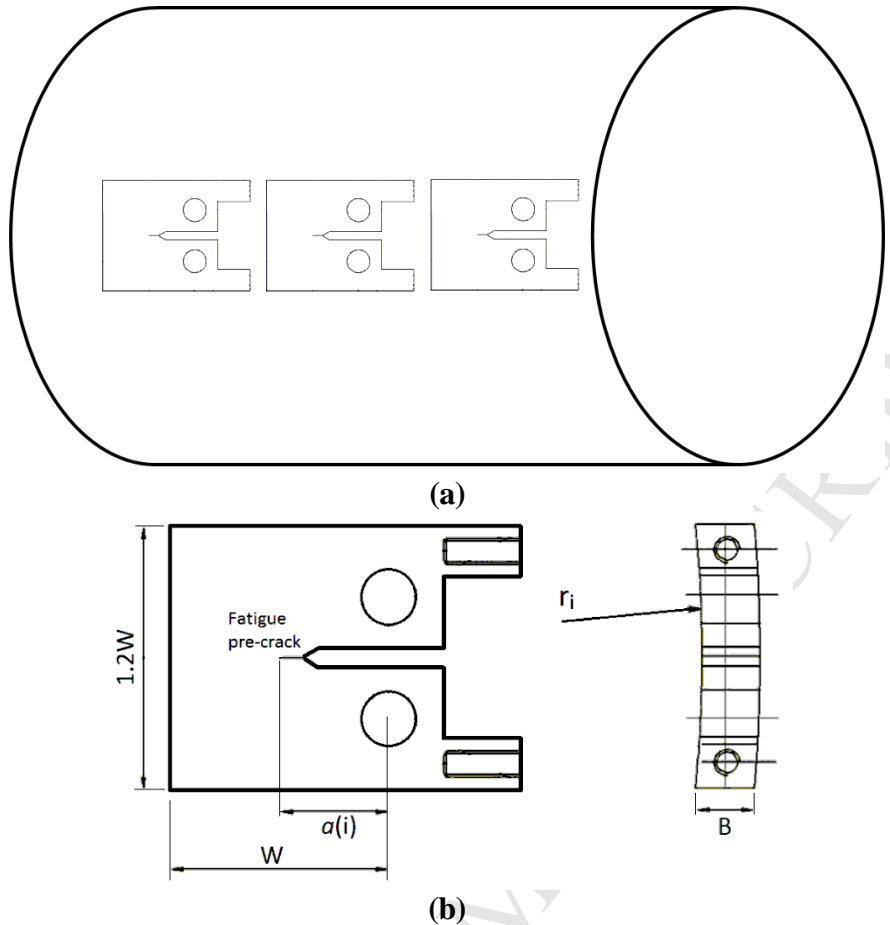
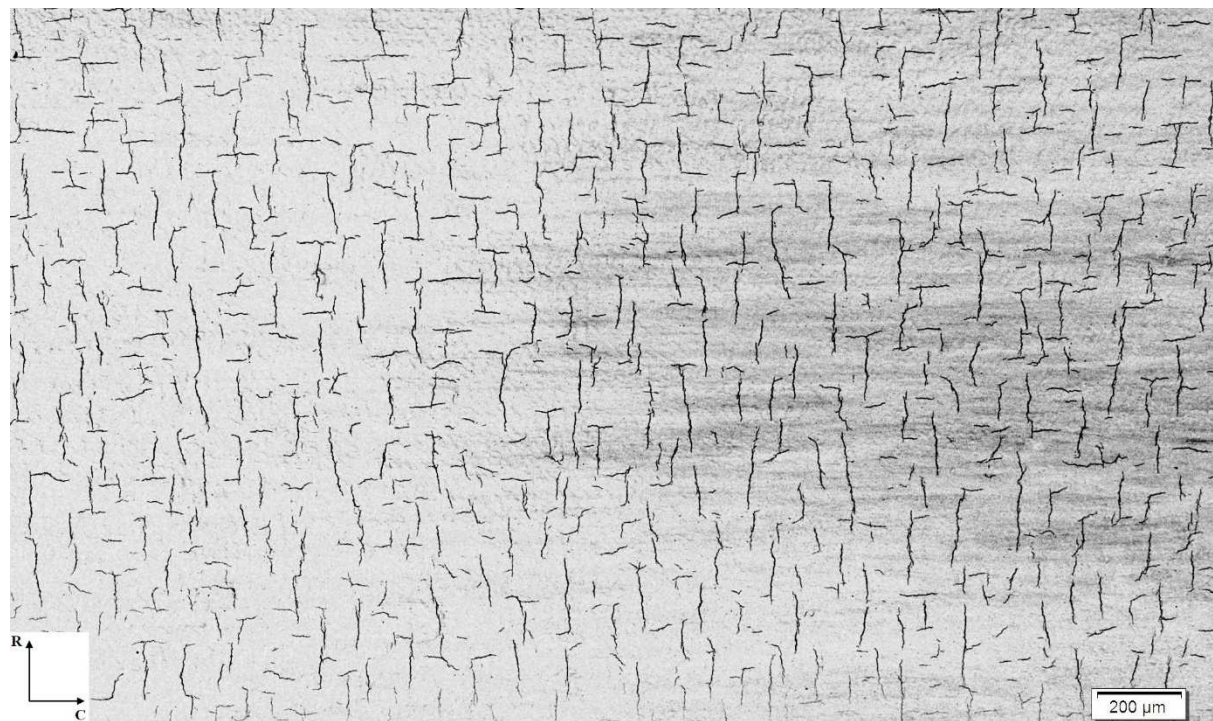
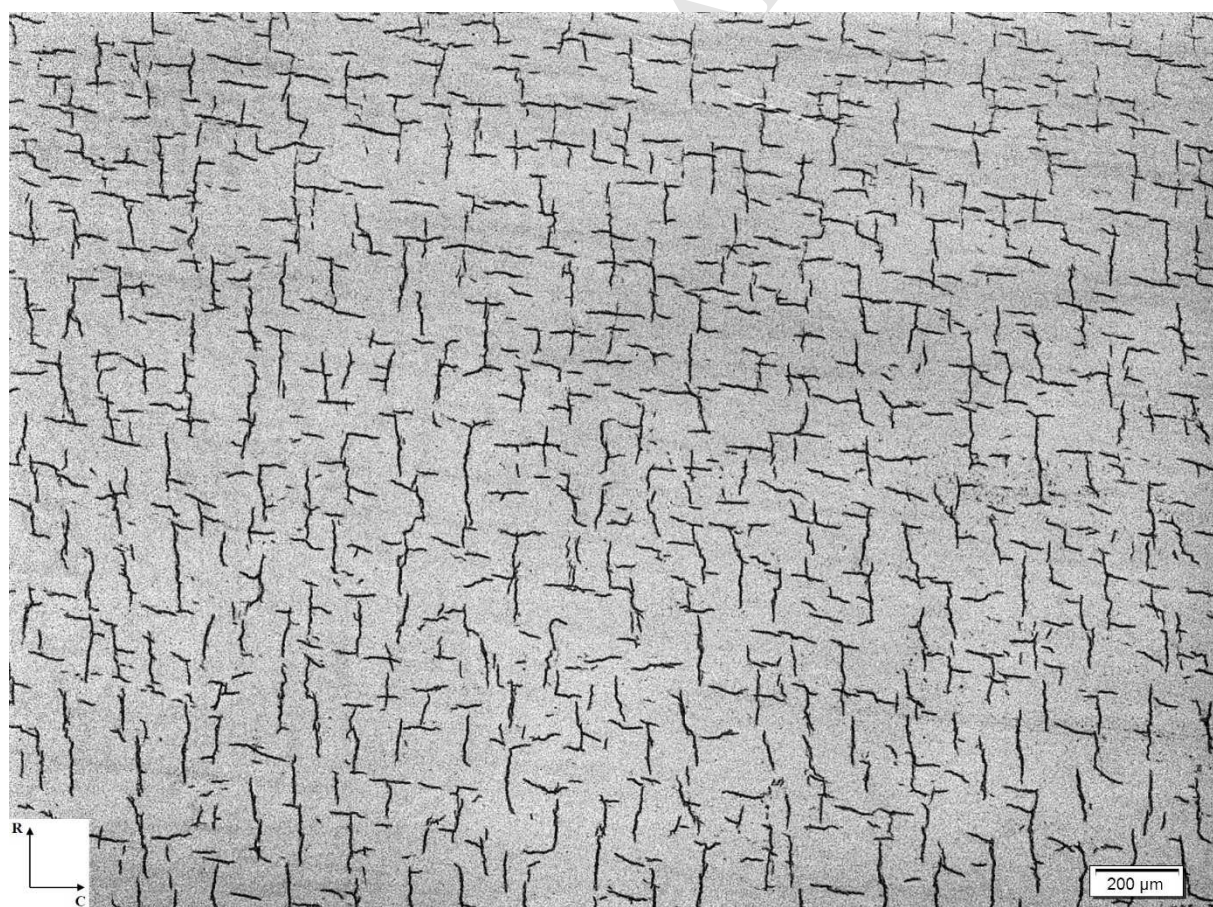


Figure 2: Schematic depicting (a) orientation of CCT specimens wire cut from Zr-2.5%Nb PT spool and (b) details of CCT specimens



(a)



(b)



(c)

Figure 3: Optical micrograph depicting hydride morphology along radial-circumferential plane of Zr-2.5%Nb alloy PT spool after charging 100 wppm of hydrogen, subjected to stress re-orientation and annealing heat treatment for 1 hour at (a) 300 °C, (b) 325 °C and (c) 350 °C temperature.

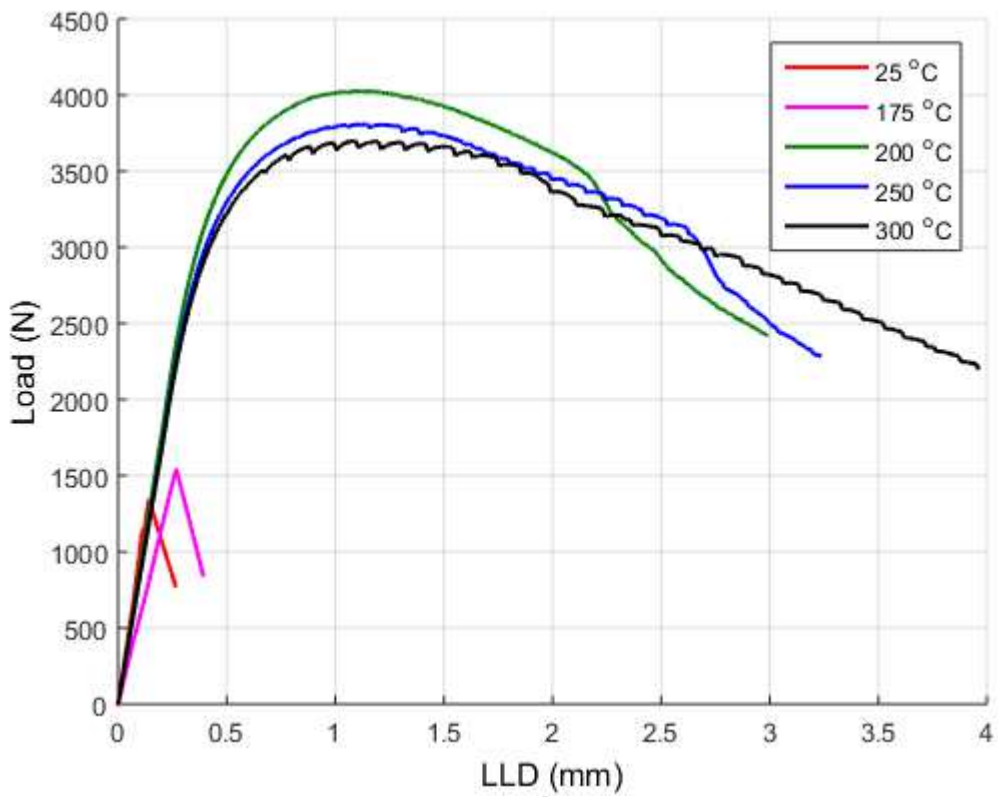


Figure 4a: [AN300] Load vs. LLD curves of samples having partial radial hydride (stress reorientation treatment + annealing at 300 °C for 1 hour) and tested between 25 °C and 300 °C temperature. Pop-in was seen for the samples tested up to 175 °C.

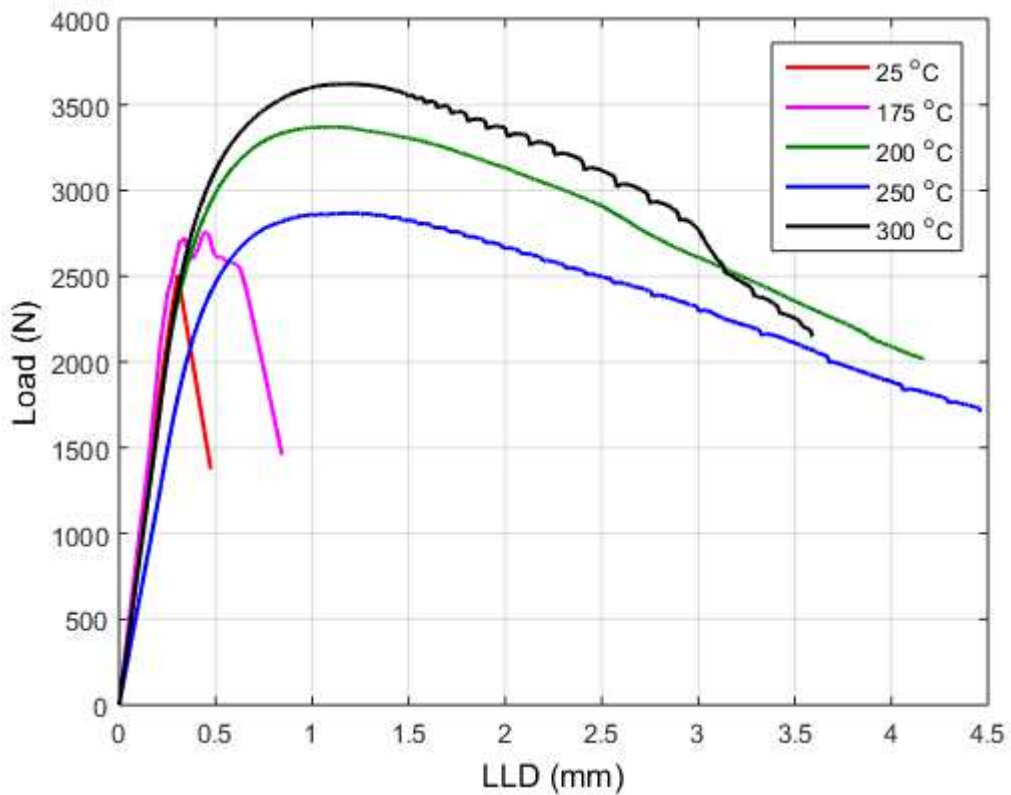


Figure 4b: [AN325] Load vs. LLD curves of samples having partial radial hydride (stress reorientation treatment + annealing at 325 °C for 1 hour) and tested between 25 °C and 300 °C temperature. Pop-in was seen for the samples tested up to 175 °C.

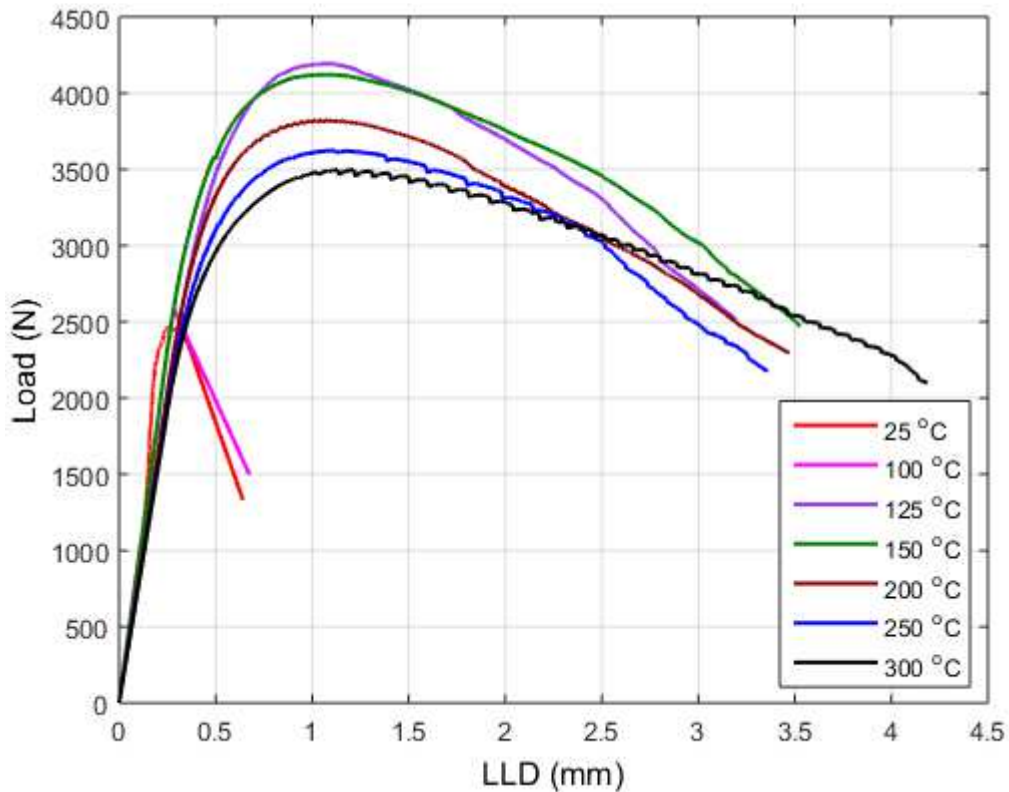


Figure 4c: [AN350] Load vs. LLD curves of samples having partial radial hydride (stress reorientation treatment + annealing at 350 °C for 1 hour) and tested between 25 °C and 300 °C temperature. Pop-in was seen for the samples tested up to 100 °C.

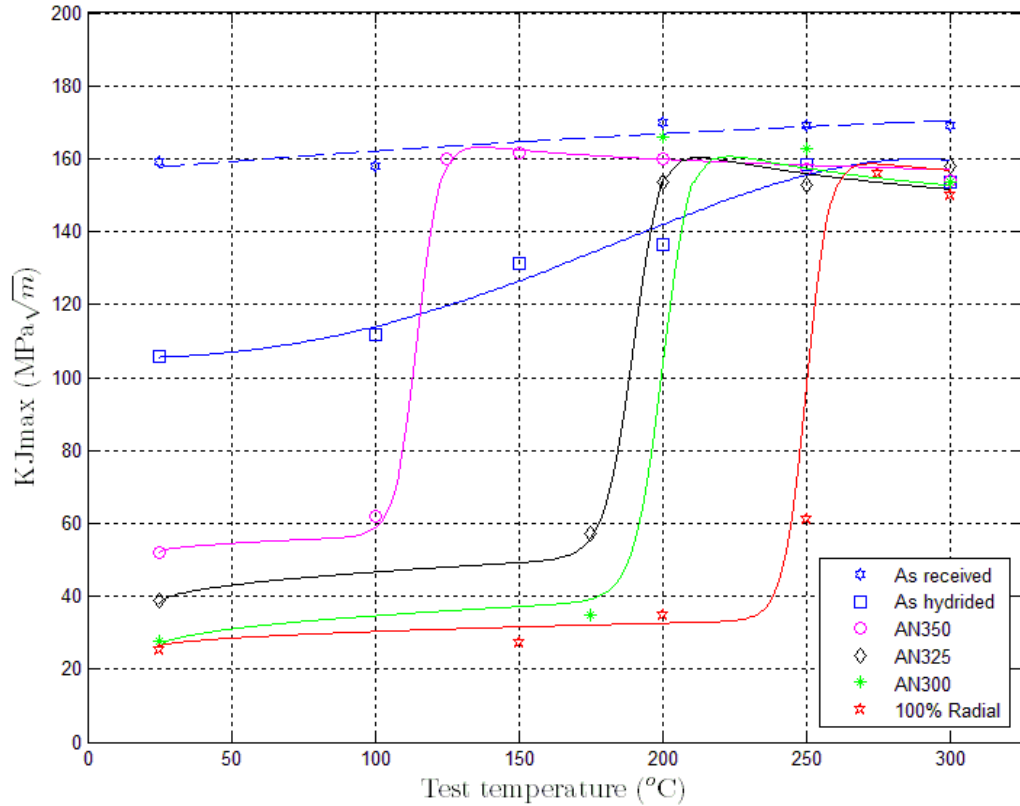


Figure 5: Behavior of fracture toughness ($K_{J\max}$) with respect to temperature for as received Zr-2.5%Nb alloy PT material (as received), having circumferential hydrides (as hydrided) and having hydrides with variable HCCs (100% Radial, AN300, AN325 and AN350).

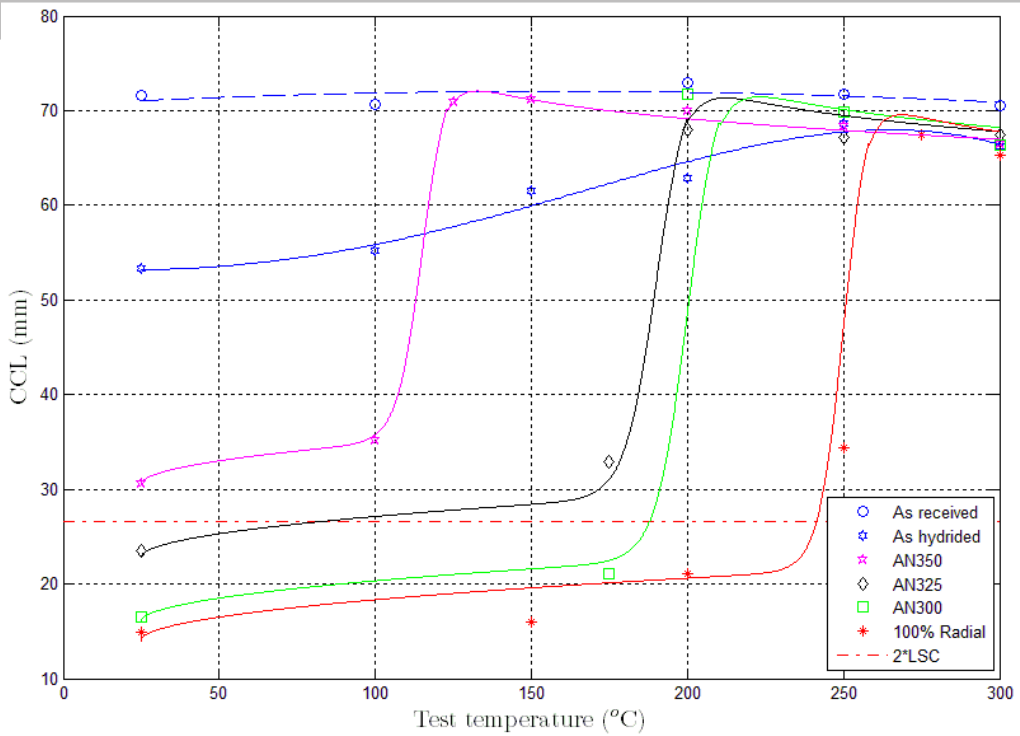


Figure 6: Critical Crack Length (CCL) behavior with respect to temperatures for as received Zr-2.5%Nb alloy PT material (as received), having circumferential hydrides (as hydrided) and having hydrides with variable HCCs (100% Radial, AN300, AN325 and AN350).

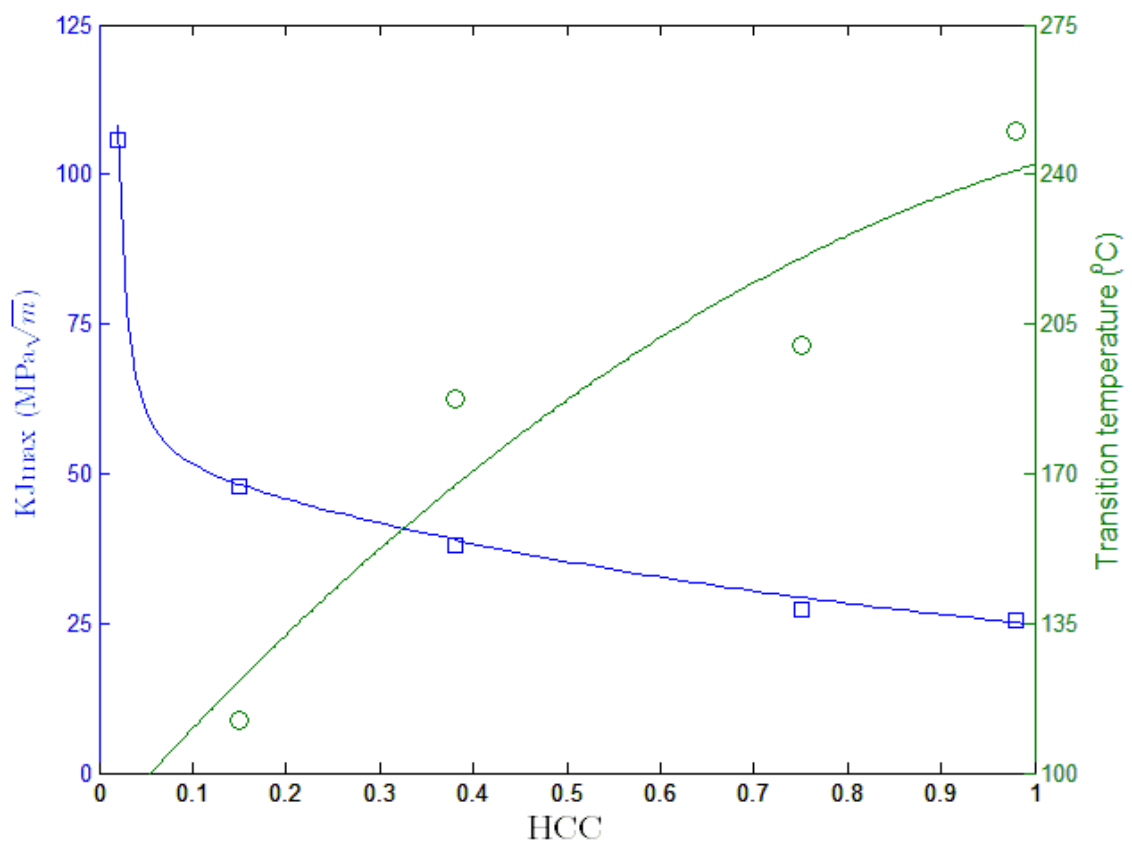
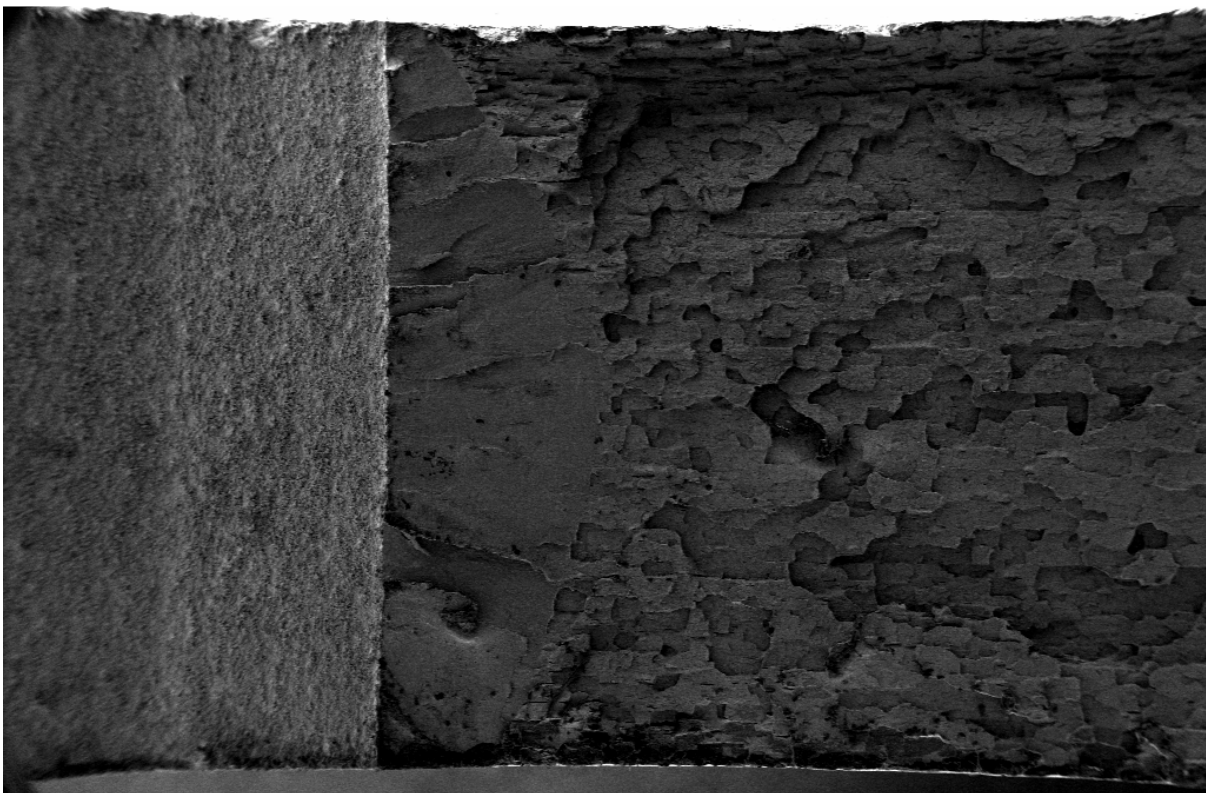
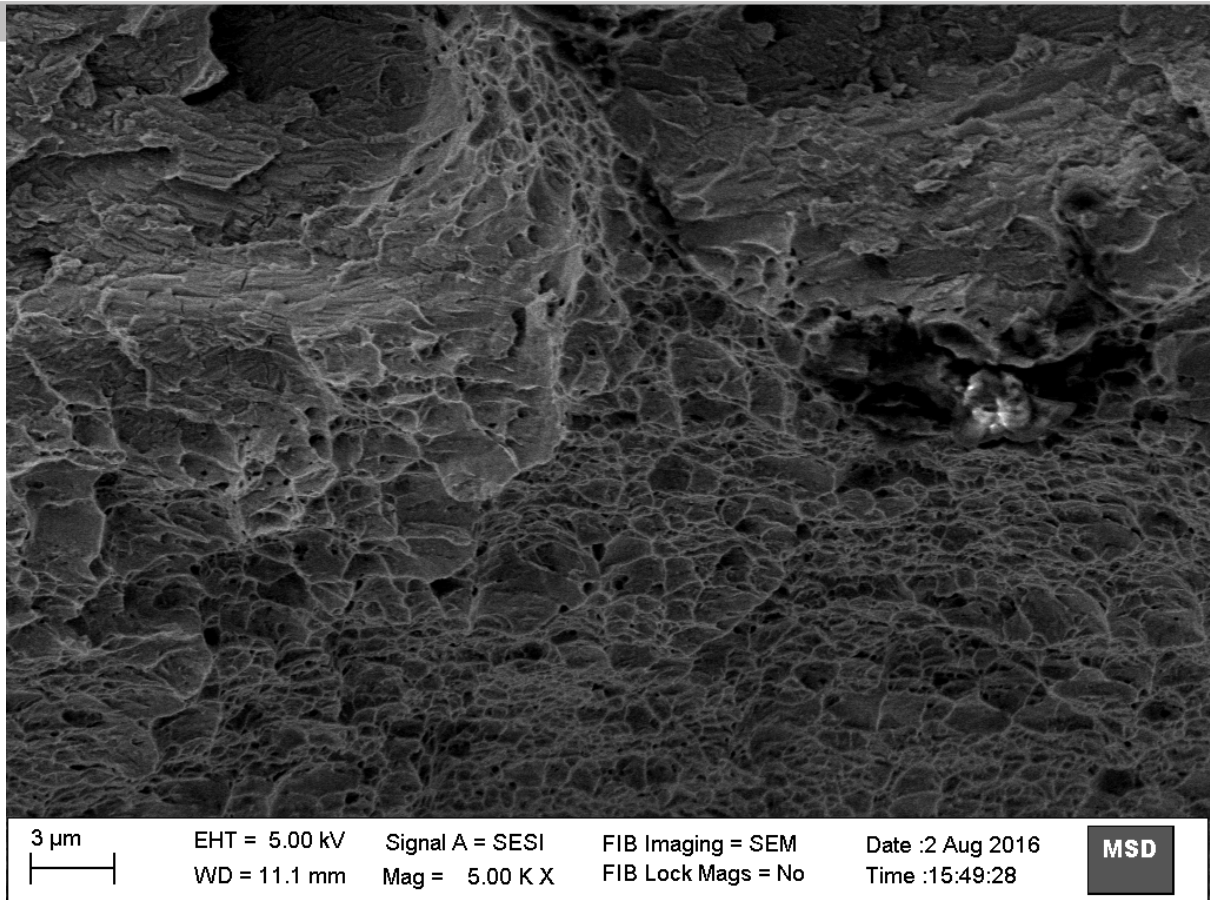


Figure 7: Plot of room temperature fracture toughness ($K_{J\max}$) and transition temperature with respect to different HCCs.

100 µm
HEHT = 5.00 kV
WD = 11.5 mmSignal A = SESI
Mag = 37 XFIB Imaging = SEM
FIB Lock Mags = NoDate : 2 Aug 2016
Time : 15:43:39

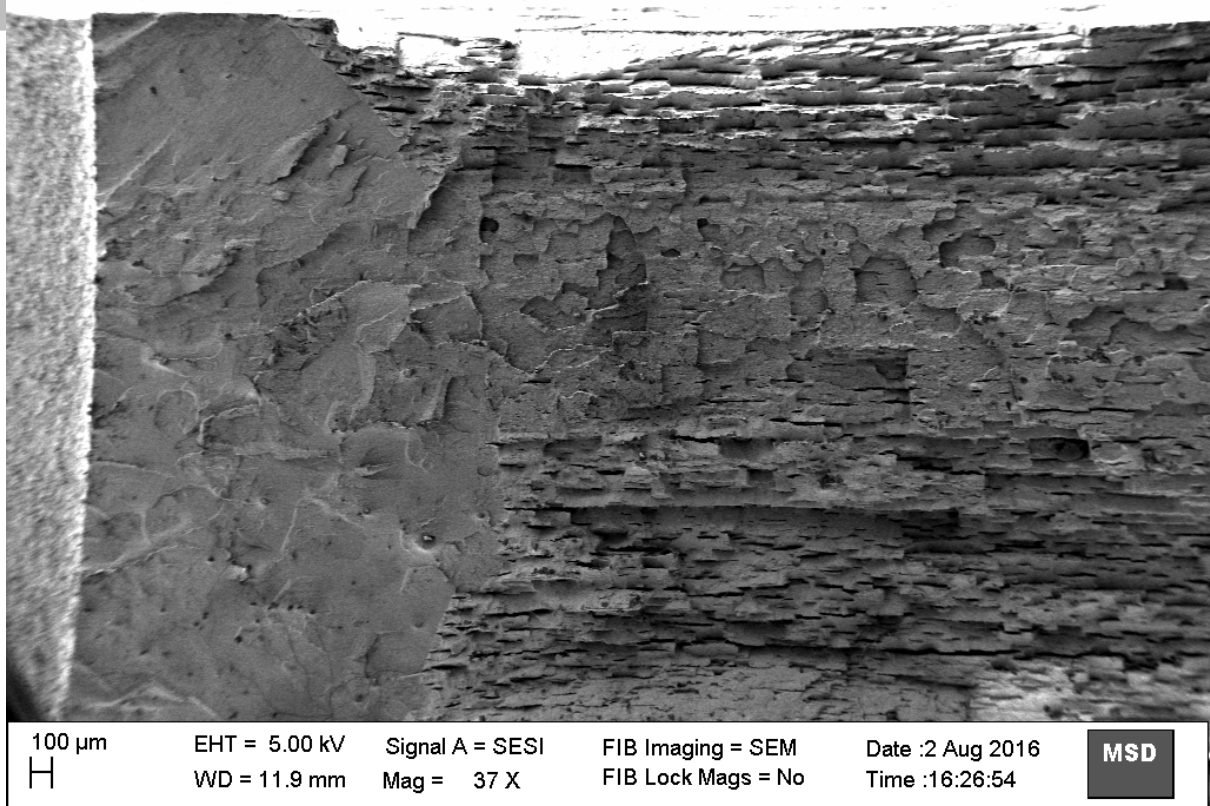
MSD

(a)

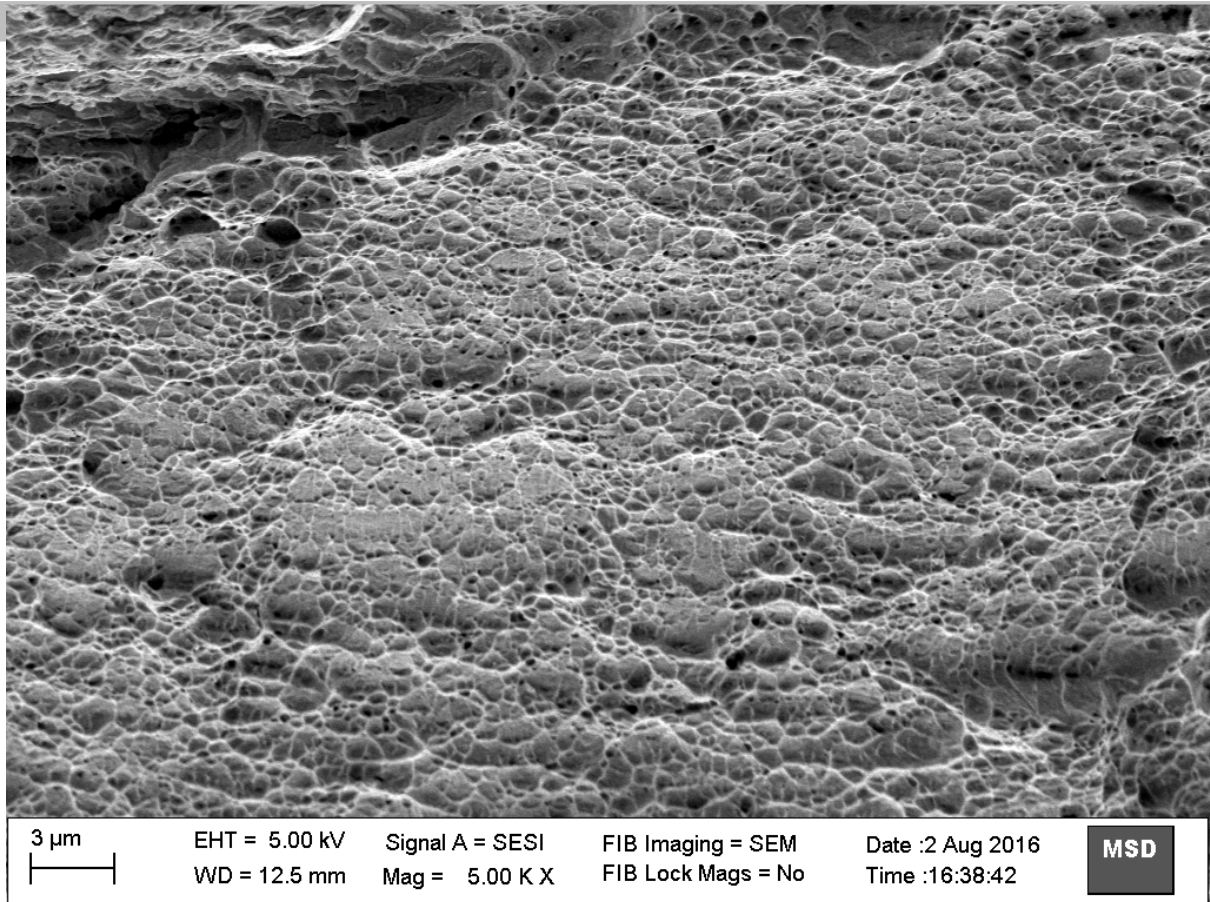


(b)

Figure 8: SEM fractographs of Zr-2.5%Nb alloy PT material having partial radial hydrides (AN300) for fracture testing at ambient temperature. Crack growth direction is from left to right. Small size and distant zones of ductile tearing were seen on the fracture surface (a) lower magnification and (b) higher magnification.



(a)



(b)

Figure 9: SEM fractographs of Zr-2.5%Nb alloy PT material having partial radial hydrides (AN350) for fracture testing at room temperature. Crack growth direction is from left to right. Big size and densely populated zones of ductile tearing features were seen on the fracture surface (a) lower magnification and (b) higher magnification.

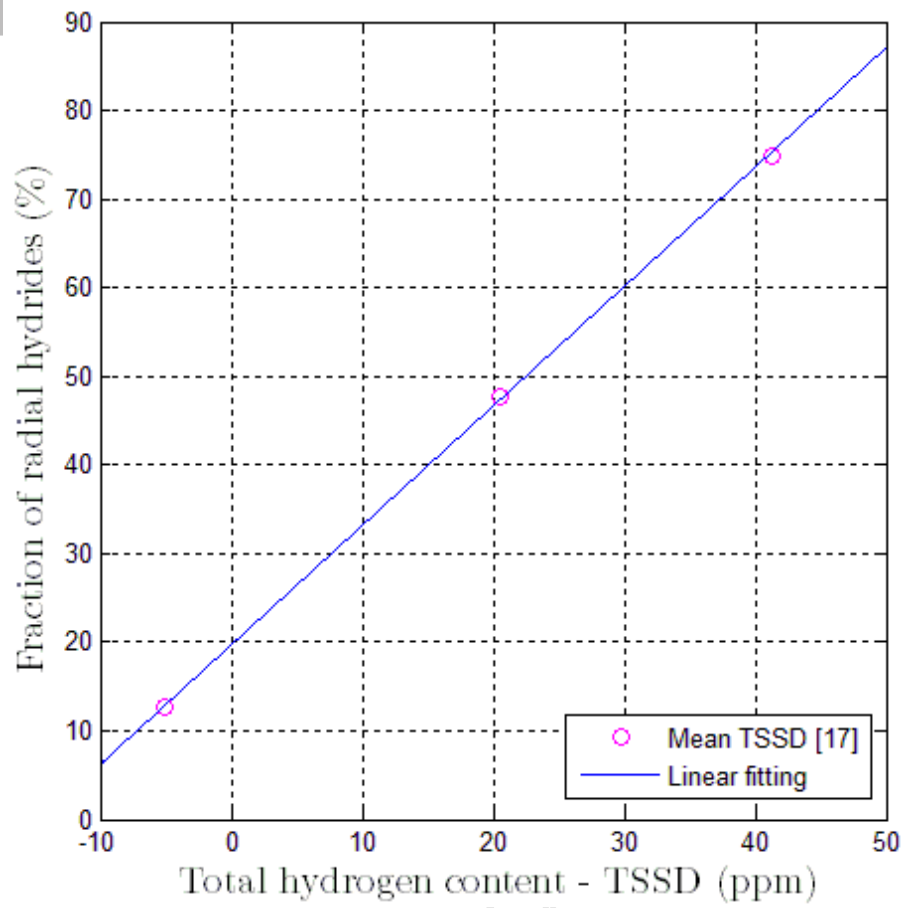


Figure 10: Plot of fraction of radial hydride and (total hydrogen content – TSSD) for various annealing heat treatment temperatures